

Simon W. M. Tanley,
Laurina-Victoria Starkey,
Lucinda Lamplough, Surasek
Kaenket and John R. Helliwell*

School of Chemistry, Faculty of Engineering and
Physical Sciences, University of Manchester,
Brunswick Street, Manchester M13 9PL, England

Correspondence e-mail:
john.helliwell@manchester.ac.uk

Received 2 April 2014

Accepted 14 June 2014

PDB references: 4owh; 4owc

The binding of platinum hexahalides (Cl, Br and I) to hen egg-white lysozyme and the chemical transformation of the PtI_6 octahedral complex to a PtI_3 moiety bound to His15

This study examines the binding and chemical stability of the platinum hexahalides K_2PtCl_6 , K_2PtBr_6 and K_2PtI_6 when soaked into pre-grown hen egg-white lysozyme (HEWL) crystals as the protein host. Direct comparison of the iodo complex with the chloro and bromo complexes shows that the iodo complex is partly chemically transformed to a square-planar PtI_3 complex bound to the N^δ atom of His15, a chemical behaviour that is not exhibited by the chloro or bromo complexes. Each complex does, however, bind to HEWL in its octahedral form either at one site (PtI_6) or at two sites ($PtBr_6$ and $PtCl_6$). As heavy-atom derivatives of a protein, the octahedral shape of the hexahalides could be helpful in cases of difficult-to-interpret electron-density maps as they would be recognisable 'objects'.

1. Introduction

The platinum hexahalides (K_2PtCl_6 , K_2PtBr_6 and K_2PtI_6) each consist of an octahedral arrangement of six halogen atoms bound to a platinum centre. As heavy-atom derivatives of a protein, the octahedral shape of the platinum hexahalides make them recognisable 'objects' in initial electron-density map interpretations compared with single-point metal atoms which may not be recognisable in noisy difference Patterson or Fourier maps (Helliwell, 2013*b*). In particular, we envisage that they could become important, for example, in X-ray laser experiments that are striving to work with ever smaller samples, currently at the microcrystal/nanocrystal size but anticipated to transition to nanoclusters (see Helliwell, 2013*a*). These compounds also offer a way to solve unknown protein structures by powder diffraction involving dispersive and/or isomorphous intensity differences (Helliwell *et al.*, 2010).

K_2PtCl_6 and K_2PtBr_6 have both been studied before using soaking crystallization conditions into pre-grown hen egg-white lysozyme (HEWL) crystals; Sun and coworkers described a quick soak (~10 min) approach and test using K_2PtCl_6 (Sun *et al.*, 2002), while Helliwell and coworkers undertook a time-dependent analysis of K_2PtBr_6 binding to lysozyme studied by protein powder and single-crystal X-ray analysis (up to 3 h soak time; Helliwell *et al.*, 2010). Both of these studies showed that these complexes bound to two sites on the protein. Site 1 is on a special position in a crevice between Arg14 in two symmetry-related molecules and site 2 is close to Ser86, Lys1 and Gln41 of one molecule in a crevice next to Pro79, Asn65 and Asn74 of a symmetry-related molecule. The platinum hexaiodide is probably of most interest as the most electron-dense complex and therefore this study scrutinizes in detail the chemical behaviour of K_2PtI_6 soaked into pre-grown HEWL crystals and also whether its chemical behaviour is the same as that of K_2PtCl_6 and K_2PtBr_6 . The cases of K_2PtCl_6 and K_2PtBr_6 have also been studied under basically identical chemical and measurement conditions to the iodo form. An unexpected chemical behaviour of the iodo compound to form a PtI_3 moiety bound to the His15 N^δ atom has been observed which was not observed with the chloro or bromo forms.

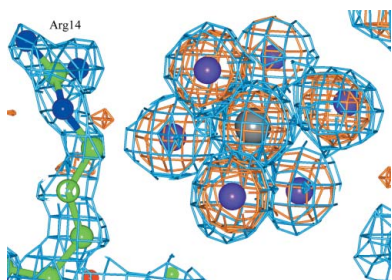


Table 1

X-ray crystallographic data and final protein model-refinement statistics for HEWL crystals soaked in K_2PtI_6 .

Values in parentheses are for the last shell.

PDB code	4owc
Data-collection temperature (K)	100
Data reduction	
Space group	$P4_32_12$
Unit-cell parameters (Å)	$a = b = 78.69, c = 36.94$
Crystal-to-detector distance (mm)	50
Observed reflections	135236
Unique reflections	14174
Resolution (Å)	27.82–1.62 (1.65–1.62)
Completeness (%)	97.8 (79.0)
R_{merge} (%)	0.0893 (0.1779)
$\langle I/\sigma(I) \rangle$	16.2 (3.7)
Multiplicity	8.7 (2.4)
Refinement	
Cruickshank DPI (Å)	0.09
No. of atoms	
Protein atoms	1001
Water molecules	105
Pt and halogen atoms	14
Other bound molecules or ions†	1
Average B factors (Å ²)	
Protein atoms	16.6
Water molecules	23.3
Pt and halogen atoms	16.8
Other bound molecules or ions†	11.5
R factor/ R_{free} (%)	17.4/19.3
R.m.s.d., bonds (Å)/angles (°)	0.02/1.81
Ramachandran values (%)	
Most favoured	96.1
Additional allowed	3.9
Disallowed	0

† The other bound atom to the protein is an Na ion.

2. Methods

2.1. Crystallization conditions

HEWL crystals were prepared using a batch method as outlined by Blundell & Johnson (1976). 60 mg HEWL was dissolved in 1 ml 0.04 M acetate buffer pH 4.7 and 1 ml 10% NaCl was added to the solution. HEWL crystals were then soaked for 24 h in a 10 mM solution of either K_2PtCl_6 , K_2PtBr_6 or K_2PtI_6 . Each heavy-atom compound solution was obtained from a pre-made stock solution at 50 mM in acetate buffer.

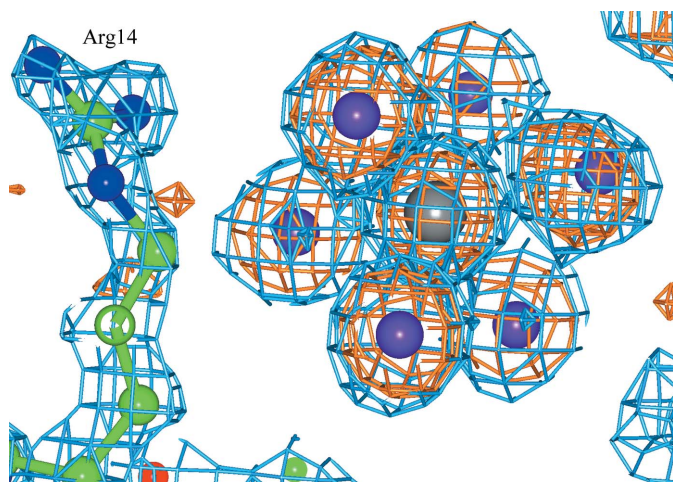


Figure 1
 PtI_6 binding in a special position between two Arg14 residues in symmetry-related molecules. The $2F_o - F_c$ electron-density map (blue) and the anomalous difference electron-density map (orange) are shown. The Pt atom is in grey and I atoms are in purple.

2.2. X-ray diffraction data collection, protein structure solution and model refinement

A crystal from each soaking condition was scooped into a loop using Paratone as a cryoprotectant. All X-ray diffraction (XRD) data were measured on a Bruker APEX II home-source diffractometer at an X-ray wavelength of 1.5418 Å and a fixed temperature of 100 K (Table 1). The XRD data-collection strategy used led to a high completeness of unique data, high anomalous difference completeness and a reasonable level of data redundancy. All XRD data were processed using the *PROTEUM2* software package (Bruker AXS, Madison, WI, USA).

The crystal structures were solved using *Phaser* (McCoy *et al.*, 2007) followed by rigid-body and restrained refinement with *REFMAC5* in *CCP4* (Murshudov *et al.*, 2011), using the previously reported lysozyme structure with PDB code 2w1y as the molecular search model (Cianci *et al.*, 2008). The use of *Phaser* was probably not required as 2w1y is relatively isomorphous to these crystals. Model building, adjustment and refinement were carried out using *Coot* (Emsley & Cowtan, 2004) and *REFMAC5* (Murshudov *et al.*, 2011) in *CCP4*. Ligand-binding occupancies were calculated using *SHELXL* (Sheldrick, 2008). The crystallographic and molecular model-refinement parameters for K_2PtI_6 are summarized in Table 1 and those for K_2PtCl_6 and K_2PtBr_6 are given in Supplementary Table S1¹. All figures were produced using *CCP4mg* (McNicholas *et al.*, 2011).

3. Results

3.1. HEWL + K_2PtI_6

The binding of PtI_6 to HEWL shows both similarities and differences to the previous studies involving $PtCl_6$ (Sun *et al.*, 2002) and $PtBr_6$ (Helliwell *et al.*, 2010). PtI_6 binds to site 1, a crevice between two Arg14 residues in symmetry-related molecules (Fig. 1). This site is located at a special position, with a twofold axis passing through the Pt atom and two iodines. Individually refined heavy-atom occupancies, as well as whole group refined occupancies, are given in Supplementary Tables S2–S4 for each hexahalide complex. An octahedral PtI_6 molecule is not bound in site 2, a crevice between Ser86, Lys1 and Gln41 of chain *A* next to Pro79, Asn65 and Asn74 of a symmetry-related molecule. Most interestingly, there is a new binding site that is chemically distinct comprising a PtI_3 moiety bound to the N^δ atom of His15, forming a square-planar complex (Fig. 2).

3.2. HEWL + K_2PtBr_6 and HEWL + K_2PtCl_6

The $PtBr_6$ and $PtCl_6$ complexes again showed binding at two sites on the HEWL protein as seen in the previously published short soaking studies of 10 min and 3 h with HEWL (Sun *et al.*, 2002; Helliwell *et al.*, 2010). However, no binding to His15 was observed for these complexes in this or the previous studies.

4. Discussion

Of most novel interest is the PtI_3 moiety bound to His15. This is reminiscent of Zeise's salt ($PtCl_3C_2H_4$; Black *et al.*, 1969). This also seems to be somewhat similar, but not identical, to the results of Messori *et al.* (2013), who soaked $PtI_2(NH_3)_2$ into pre-grown HEWL crystals for two months in DMSO medium; they described a

¹ Supporting information has been deposited in the IUCr electronic archive (Reference: NO5054).

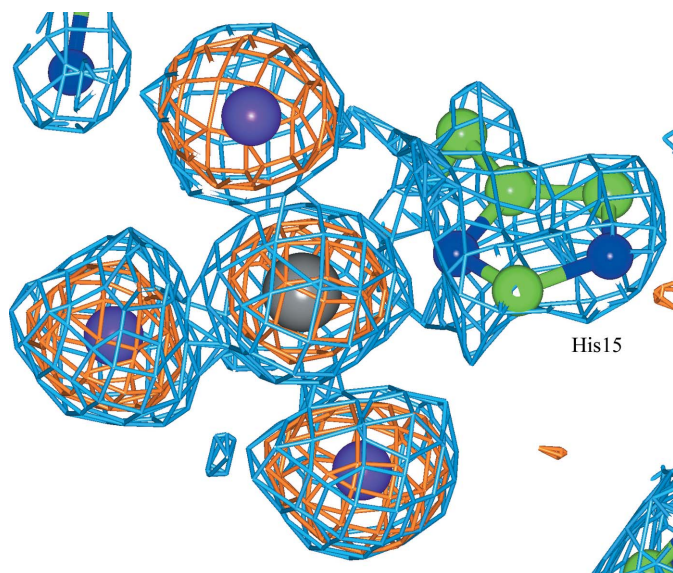


Figure 2
A PtI_3 moiety bound to the N^δ atom of His15. The $2F_o - F_c$ electron-density map (blue) and the anomalous difference electron-density map (orange) are shown. The Pt atom is in grey and I atoms are in purple.

$\text{PtI}_2(\text{NH}_3)$ molecule alternating between two different binding modes.

In our companion study (Tanley & Helliwell, 2014) of cisplatin and carboplatin binding to HEWL in NaI crystallization conditions, both cisplatin and carboplatin were partially converted to transiodoplatin bound at the N^δ binding site of His15. This is also similar to the results that we obtained under NaBr crystallization conditions for carboplatin (Tanley *et al.*, 2014) and cisplatin (Tanley & Helliwell, 2014) and in NaCl conditions, where carboplatin was partially converted to cisplatin (Tanley *et al.*, 2013).

We have also seen a PtI_3X moiety bound to a symmetry-related molecule in the cisplatin and carboplatin NaI conditions, as shown by three anomalous difference electron-density peaks bound to the Pt centre (Tanley & Helliwell, 2014).

5. Conclusions

For the octahedral PtI_6 hexahalide molecule bound to HEWL, we see a chemical transformation to a square-planar PtI_3 moiety bound to the N^δ atom of His15. This showed a different chemical behaviour to that of either the PtBr_6 or the PtCl_6 hexahalide complexes.

For the anticipated use with the X-ray laser, and other possible challenging-to-interpret electron-density map situations, as described in §1, PtI_6 preserved its octahedral shape at one binding site but also appeared as a chemically transformed square-planar PtI_3 moiety bound to a histidine N atom. This is acceptable of course when interpreting an electron-density map, but one has to know in advance that a complex of this shape is to be looked out for as well as an octahedron.

6. Related literature

The following references are cited in the Supporting Information for this article: Moreno-Gordaliza *et al.* (2009, 2010).

JRH is grateful to the University of Manchester for general support, to the EPSRC for a PhD studentship to SWMT, to the Thailand Government for studentship support to SK, to the School of Chemistry for crystallization and computing facilities and to the Faculty of Life Sciences for X-ray diffraction facilities.

References

- Black, M., Mais, R. H. B. & Owston, P. G. (1969). *Acta Cryst.* **B25**, 1753–1759.
- Blundell, T. L. & Johnson, L. N. (1976). *Protein Crystallography*. London: Academic Press.
- Cianci, M., Helliwell, J. R. & Suzuki, A. (2008). *Acta Cryst.* **D64**, 1196–1209.
- Emsley, P. & Cowtan, K. (2004). *Acta Cryst.* **D60**, 2126–2132.
- Helliwell, J. R. (2013a). *Science*, **339**, 146–147.
- Helliwell, J. R. (2013b). *Acta Cryst.* **A69**, s144.
- Helliwell, J. R., Bell, A. M. T., Bryant, P., Fisher, S., Habash, J., Helliwell, M., Margiolaki, I., Kaenket, S., Watier, Y., Wright, J. P. & Yalamanchilli, S. (2010). *Z. Kristallogr.* **225**, 570–575.
- McCoy, A. J., Grosse-Kunstleve, R. W., Adams, P. D., Winn, M. D., Storoni, L. C. & Read, R. J. (2007). *J. Appl. Cryst.* **40**, 658–674.
- McNicholas, S., Potterton, E., Wilson, K. S. & Noble, M. E. M. (2011). *Acta Cryst.* **D67**, 386–394.
- Messori, L., Marzo, T., Gabbiani, C., Valdes, A. A., Quiroga, A. G. & Merlino, A. (2013). *Inorg. Chem.* **52**, 13827–13829.
- Moreno-Gordaliza, E., Cañas, B., Palacios, M. A. & Gómez-Gómez, M. M. (2009). *Anal. Chem.* **81**, 3507–3516.
- Moreno-Gordaliza, E., Cañas, B., Palacios, M. A. & Gómez-Gómez, M. M. (2010). *Analyst*, **135**, 1288–1298.
- Murshudov, G. N., Skubák, P., Lebedev, A. A., Pannu, N. S., Steiner, R. A., Nicholls, R. A., Winn, M. D., Long, F. & Vagin, A. A. (2011). *Acta Cryst.* **D67**, 355–367.
- Sheldrick, G. M. (2008). *Acta Cryst.* **A64**, 112–122.
- Sun, P. D., Radaev, S. & Kattah, M. (2002). *Acta Cryst.* **D58**, 1092–1098.
- Tanley, S. W. M., Diederichs, K., Kroon-Batenburg, L. M. J., Levy, C., Schreurs, A. M. M. & Helliwell, J. R. (2014). *Acta Cryst.* **F70**, 1135–1142.
- Tanley, S. W. M., Diederichs, K., Kroon-Batenburg, L. M. J., Schreurs, A. M. M. & Helliwell, J. R. (2013). *J. Synchrotron Rad.* **20**, 880–883.
- Tanley, S. W. M. & Helliwell, J. R. (2014). *Acta Cryst.* **F70**, 1127–1131.